

Wavelet Based Qualitative Assessment of Femur Bone Strength Using Radiographic Imaging

Sundararajan Sangeetha, Joseph Jesu Christopher, and Swaminathan Ramakrishnan

Abstract—In this work, the primary compressive strength components of human femur trabecular bone are qualitatively assessed using image processing and wavelet analysis. The Primary Compressive (PC) component in planar radiographic femur trabecular images (N=50) is delineated by semi-automatic image processing procedure. Auto threshold binarization algorithm is employed to recognize the presence of mineralization in the digitized images. The qualitative parameters such as apparent mineralization and total area associated with the PC region are derived for normal and abnormal images. The two-dimensional discrete wavelet transforms are utilized to obtain appropriate features that quantify texture changes in medical images. The normal and abnormal samples of the human femur are comprehensively analyzed using Harr wavelet. The six statistical parameters such as mean, median, mode, standard deviation, mean absolute deviation and median absolute deviation are derived at level 4 decomposition for both approximation and horizontal wavelet coefficients. The correlation coefficient of various wavelet derived parameters with normal and abnormal for both approximated and horizontal coefficients are estimated. It is seen that in almost all cases the abnormal show higher degree of correlation than normals. Further the parameters derived from approximation coefficient show more correlation than those derived from the horizontal coefficients. The parameters mean and median computed at the output of level 4 Harr wavelet channel was found to be a useful predictor to delineate the normal and the abnormal groups.

Keywords—Image processing, planar radiographs, trabecular bone and wavelet analysis.

I. INTRODUCTION

ASSESSMENT of mechanical strength of bone remains a central issue in biomechanics. The architecture of the bone is composed of the cortical bone shell and trabecular bone core. Trabecular bone is a spongy, porous type found at the ends of all bones, such as pelvis and spine [1]. In proximal femur, trabecular bone forms a pattern of net-like strands varying in thickness and number [2]. It has a complex three-dimensional structure consisting of struts and plates.

S. Sangeetha, Research Scholar, Madras Institute of Technology, Chennai 600044, India (e-mail: s.sangeethame@gmail.com).

J. Jesu Christopher, Research Scholar, Madras Institute of Technology, Chennai 600044, India (e-mail: jesu_jakson@yahoo.co.in)

S. Ramakrishnan, Assistant Professor is with the Instrumentation Engineering Department, Madras Institute of Technology, India (e-mail: ramki@mitindia.com).

Trabecular bone is a dynamic system and its architecture can adaptively compensate for local deficiencies in strength through remodeling or micro modeling [3]. Many lines of evidence indicate that the decreased bone strength characteristic of osteoporosis is dependent not only on BMD, but also on trabecular bone microarchitecture [4], [5] and mineralization [6]. The correlation between bone strength and bone mass is well established but the relationship between trabecular microarchitecture and biomechanical properties are less explored [7], [8].

Bone mineral density is usually assessed using Dual Energy X-ray Absorptiometry (DEXA) [9], Radiographic Absorptiometry (RA) [10], [11] or Computed Tomography (CT) equipments [9]. Although these techniques generate three-dimensional data, radiographic images using film or digital images provide the most common mode of assessment in orthopedic units. The significant parts of the information that are available in 3D images are also available in the conventional radiograph [12]. Further, digital imaging and digital image processing techniques are new developments which increase the diagnostic value of radiographs [13], [14]. Hence, there has been considerable interest in using conventional radiography combined with various image and texture analysis techniques for assessing trabecular structure [15].

Recently, methods based on multiresolution or multichannel analysis such as wavelet transform has been introduced for characterizing texture properties. They outperform most traditional single resolution techniques which fail to characterize textures with different resolutions effectively. Wavelet provides a precise and unified framework for spatial scale analysis. This tool has already and successfully been proposed for texture analysis using wavelet packets [16] and wavelet frames [17]. The first technique leads to adaptive wavelet decomposition while the second yields a description of translation invariant. Wavelet analysis is successfully used in functional medical imaging and finds wide application with MR imaging [18]. An application of wavelet-based texture analysis has been also reported for several biological structures [19], [20].

In this work, primary compressive strength component of human femur trabecular bone in radiographic images were analyzed using wavelets. The processed normal and abnormal images were decomposed at level 4 using Harr wavelet and the statistical parameters that characterize the texture features were derived for analysis.

II. METHODOLOGY

Digitized pelvis images (N=50, Normal 25, Abnormal 25), recorded using clinical x-ray unit (Siemens 500mA Polyscope) were considered for the study. The exposures were made with 160 mAs at 60 kVp and exposure time was 0.05s. The standard anteroposterior view was used to image all subjects and the recorded radiographs were digitized using an AGFA digitizer. The proximal femur bone with constant resolution of image size 300 x 350 was cropped from the digitized pelvis images. Auto threshold binarization algorithm was employed to recognize the presence of mineralization in the digitized images by considering the neighborhood pixels [21], [22].

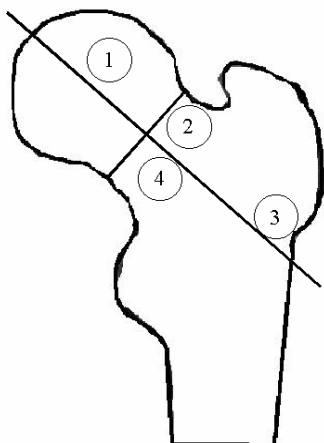


Fig. 1 Representation of various strength zones (Singh et al): Primary compressive (1)

The distributions of mineralization in primary compressive region in the binarized images were delineated as region of interest as proposed by Singh et al. [23]. The regions of interest were marked by the position of the regions described in terms of a coordinate system. The axes are shortest line across the femoral neck and a line through the center of the femoral head and midpoint of the two axes are shown in the Fig. 1. The primary supporting structure of the femoral head to be the primary compressive strut, is a dense column of trabecular bone projecting from the pressure buttress of the medial femoral neck which is the predominant load-bearing structure connecting the femoral head to the femoral neck [24].

The delineated images are then subjected to wavelet based analysis. Wavelets are the multiresolution techniques intend to transform an image into a presentation in which information regarding both the nature of the frequency components (high or low) and the location of occurrence of these frequencies in the image axis preserved. The qualitative analyses were also performed on the delineated images to derive apparent mineralization and total area. The percentage of apparent mineralization is the ratio of bone area to the total area.

For multiresolution decomposition of images, it is often desirable to differentiate the local orientation of the image features. For this purpose, a scaling function $\Phi(x, y)$, which is a lowpass filter, is introduced along with three wavelet functions $\Psi^1(x, y)$ ($1 \leq I \leq 3$) where each wavelet $\Psi^1(x, y)$

$\Psi^2(x, y)$ and $\Psi^3(x, y)$ can be interpreted as the impulse response of a bandpass filter having a specific orientation selectivity in the vertical, horizontal and diagonal directions, respectively. The low-pass and high-pass filtering actions are performed using digital filters with impulse responses G and H , (G and H form a pair of quadrature mirror filters) respectively [25]. An image $f(x, y)$ with a spatial resolution of 2^j can therefore be decomposed through level-1 using

$$\begin{aligned} f(x, y) = & A^1 \Phi_2^j(x - 2^j n, y - 2^j m) \\ & + H^1 \Psi_2^1(x - 2^j n, y - 2^j m) \\ & + V^1 \Psi_2^2(x - 2^j n, y - 2^j m) \\ & + D^1 \Psi_2^3(x - 2^j n, y - 2^j m) \end{aligned} \quad (1)$$

Where

$$A^1 = ((f(x, y), \Phi_2^j(x - 2^j n, y - 2^j m))_n, m \in Z^2) \quad (2)$$

$$H^1 = ((f(x, y), \Psi_2^1(x - 2^j n, y - 2^j m))_n, m \in Z^2) \quad (3)$$

$$V^1 = ((f(x, y), \Psi_2^2(x - 2^j n, y - 2^j m))_n, m \in Z^2) \quad (4)$$

$$D^1 = ((f(x, y), \Psi_2^3(x - 2^j n, y - 2^j m))_n, m \in Z^2) \quad (5)$$

Each of the above sequences of inner products can be considered as an image. The DWT decomposition of an image into four channels, namely A^1 , H^1 , V^1 and D^1 , involves first the convolution of the original image with impulse responses of low-pass filter G and high-pass filter H , respectively, along the rows and then columns, which produces four filtered images, each with every second sample redundant. Therefore the filter stage is followed by the process of subsampling by a factor of 2 (discarding every other sample), which reduces the size or spatial resolution of the filtered images to half the original image. Therefore level-1 DWT decomposition of an image produces a representation of the image in the form of four sub-images, where A^1 represents the spatial distribution of low-frequency components, and H^1 , V^1 and D^1 represent the spatial distribution of high-frequency components present at a resolution half that of the original image. Among the high-frequency channels, H^1 gives the horizontal edges (vertical high frequencies), V^1 gives the vertical edges (horizontal high frequencies), and D^1 gives higher frequencies in both directions (corners). This set of four images is called an orthogonal wavelet representation in two dimensions. The decomposition process can be recursively applied to the low-frequency channel A^1 to generate image details A^2 (low-frequency channel) and H^2 , V^2 and D^2 (high-frequency channels), at the next level and so on. The G and H filters are used to implement the wavelet transform [26].

III. RESULTS AND DISCUSSION

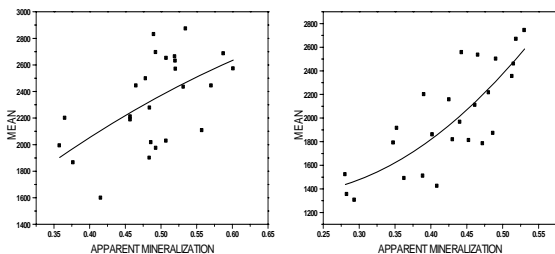
The binarized radiographic images of femur trabeculae bone is shown in Fig. 2. Fig. 2(a) is image of a normal sample whereas Fig. 2(b) is that of the abnormal. The normal trabeculae patterns are distinctly seen as they are closely organized. Characteristic discontinuities, overlaps and large spacings are seen in abnormals.



(a) Normal bone (b) Abnormal bone

Fig. 2 Binary image representation of Trabeculae bone

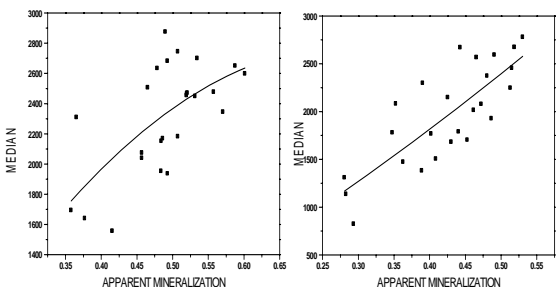
The normal and abnormal images of femur trabecular bone are analyzed using Harr wavelet. The statistical parameters such as mean, median, mode, standard deviation, mean absolute deviation and median absolute deviation are estimated at level 4 decomposition for both approximation and horizontal wavelet coefficients.



(a) Normal bone (b) Abnormal bone

Fig. 3 Variations of mean with apparent mineralization in primary compressive component of normal and abnormal samples

The scattergram showing the variation in mean derived from approximation coefficient with apparent mineralization in primary compressive strength component region for normal and abnormal samples are shown in the Fig. 3(a) and 3(b) respectively. Although there is a linear relationship it is found that the correlation coefficient for a normal sample is 0.56321. This could be attributed to large variation in apparent percentage mineralization among normals. In the case of abnormal, the correlation coefficient of mean with apparent mineralization is higher than the normal samples.



(a) Normal bone (b) Abnormal bone

Fig. 4 Variations of median with apparent mineralization in primary compressive component of normal and abnormal samples

The scattergram showing the variation in median derived from approximation coefficient with apparent mineralization in primary compressive strength component region for normal and abnormal samples is plotted in the Fig. 4(a) and 4(b) respectively. Higher degree of linear correlation is observed for both the cases. Correlation was more in abnormal than normals.

The correlation coefficient of various wavelet derived parameters with normal and abnormal for both approximated and horizontal coefficients is estimated and is shown in Table I. It is seen that in almost all cases the abnormal show higher degree of correlation than normals. Further the parameters derived from approximation coefficient show more correlation than those derived from the horizontal coefficients. Among all the parameters mode, standard deviation, mean absolute deviation and median absolute deviation show poor degrees of correlation. Thus the parameters mean and median derived from approximated coefficients seems to be useful parameters to differentiate normals and abnormal.

TABLE I
CORRELATION COEFFICIENT OF VARIOUS WAVELET DERIVED PARAMETERS WITH NORMAL AND ABNORMAL FOR BOTH APPROXIMATED AND HORIZONTAL COEFFICIENTS

Statistical Parameters Derived from Harr Wavelet	Approximated Coefficient		Horizontal Coefficient	
	Normal	Abnormal	Normal	Abnormal
Mean	0.56321	0.79696	0.29576	0.42406
Median	0.64692	0.79723	0.2685	0.11166
Mode	0.24093	0.7793	0.38509	0.32944
standard deviation	0.29346	0.60502	0.60473	0.35091
median ab dev	0.37547	0.4713	0.53821	0.22336
mean ab dev	0.32606	0.58403	0.67761	0.31957

IV. CONCLUSION

Characterization of the trabecular structural properties appears to be an important adjunct to the measurement of bone mass in determining fracture risk with greater accuracy [27]. Using histological and stereological analysis, it has been shown that, by combining structural features with bone density, nearly all of the variability in mechanically measured Young's moduli could be explained [28]. However, the evaluation of bone structure, by non-invasive procedures, remains a difficult issue [29]. Over the last several years, different imaging techniques have been developed and optimized for the reconstruction of trabecular bone structure both in vitro and in vivo [30]. The development of image analysis techniques for the characterization of the 3D-trabecular bone structure remains a privileged research field [31].

The percentage mineralization in primary compressive regions is found to be uniformly high in all the images, which indicate that primary compressive is the principle strength component of the human femur bone and is in agreement with the earlier results. Mineralization is found to be high in normal images as the observed median and mode is high. Thus it appears that the region specific statistical parameters are useful

to identify strength and weakness of femur bone from planar radiographic images. To conclude, trabecular patterns appear in the proximal part of the human femur is capable of estimating fracture risk and can be reliably measured by wavelet analysis. It may also be possible to use trabecular texture in conjunction with clinical data to further increase the efficacy of fracture risk estimation. Moreover this procedure can also be automated to enhance the diagnosis without much human intervention, which would be useful for mass screening of osteoporosis and bone mass disorders.

In this study, trabecular structure and its mechanical strength distribution on human femur bone are analyzed using planar radiographs and wavelet analyses. Acquired digital images of proximal femur trabecular bone are subjected to auto threshold binarization to minimize the irregularities in images due to uneven exposure conditions. From the binarized image primary compressive strength components are delineated and the corresponding structural and statistical parameters are estimated.

In this work the normal and abnormal samples of the human femur is comprehensively analyzed using Harr wavelet. The six statistical parameters such as mean, median, mode, standard deviation, mean absolute deviation and median absolute deviation are derived at level 4 decomposition for both approximation and horizontal wavelet coefficients. The parameters derived from approximation coefficient show more correlation than horizontal coefficients. It is found that better correlation is observed for abnormal samples. The parameters mean and median computed at the output of level 4 Harr wavelet channel was found to be a useful predictor to delineate the normal and the abnormal groups.

REFERENCES

- [1] Tony M.K, Elise F.M, Glen L.N, Oscar C.Y, "Biomechanics of trabecular bone," *Annual Review of Biomedical Engineering*, Vol. 3, pp. 307-333 , 2001.
- [2] Smyth P.P, Adams J.E., Whitehouse R.W. and Taylor C. J, "Application of computer texture analysis to the Singh index," *The British Journal of Radiology*, Vol. 70, pp. 242-247, 1997.
- [3] Erben R.G, "Trabecular and endocortical bone surfaces in the rat :Modeling or remodeling," *Anatomical Record*, Vol. 246, pp. 39-46, 1996.
- [4] Lespessailles E, Chappard C, Bonnet N, Benhamou C. L, "Imaging techniques for evaluating bone microarchitecture," *Joint bone spine*, Vol.73 (3), pp.254-61, 2006.
- [5] Martin R. B, "Determinants of the mechanical properties of bones," *Journal of Biomechanics*, Vol. 24, pp. 79-88, 1991 *Biomechanics*, Vol. 24, pp. 79-88, 1991.
- [6] Landis W. J, "The strength of a calcified tissue depends in part on the molecular structure and organization of its constituent mineral crystals in their organic matrix," *Bone*, Vol. 16, pp. 533-544, 1995.
- [7] Chung H. W, Wehrli F. W, Williams J. L, Wehrli S. L, "Three-dimensional nuclear magnetic resonance microimaging of trabecular bone," *Journal of Bone and Mineral Research*, Vol. 101, pp.1452-1461, 1995.
- [8] Goulet R. W, Goldstein S. A, Ciarelli M. J, Kuhn J. L, Brown M. B, Feldkamp L. A, "The relationship between the structural and orthogonal compressive properties of trabecular bone," *Journal of Biomechanics*, Vol. 27, pp.375-398, 1994.
- [9] Ebbesen E, Thomsen J, Beck-Nielsen H, Nepper-Rasmussen H, Mosekilde, "Lumbar vertebral body compressive strength evaluated by Dual energy Xray Absorptiometry, quantitative computed tomography, and ashing". *Bone*, Vol. 25, pp.713-724, 1997.
- [10] Strid K, Kalebo P, "Bone mass determination from microradiographs by computer assisted videodensitometry," *I Methodology. Acta Radiologica*, Vol. 29, pp. 611-617,1998.
- [11] Strid K, Kalebo P, "Bone mass determination from microradiographs by computer assisted videodensitometry," *II Aluminium as a reference substance. Acta Radiologica*, Vol. 29, pp. 465-472, 1998.
- [12] Luo G, Kinney J, Kaufman J, Haupt D, Chiabrera A, Siffert R, "Relationship between plain radiographic patterns and three dimensional trabecular architecture in the human calcaneus," *Osteoporosis International*, Vol. 9, pp. 339-345, 1999.
- [13] Dunn, S. M., Van der Stelt, P. F., Ponce, A., Fenesy, K. & Shah, S, "A comparison of two registration techniques for digital subtraction radiography," *Dentomaxillofac. Radiol.* 22, 77-80, 1993.
- [14] Grondahl, H. G., Grondahl, K. & Webber, R. L, "A digital subtraction technique for dental radiography," *Oral Sur. Oral Med. Oral Pathol.* 55, 96-102, 1983.
- [15] Kaufman J, Mont M, Hakim N, Ohley W, Lundahl T, Soifer T, Siffert R, "Texture analysis of radiographic trabecular patterns in diffuse osteopenia," *Transactions of Orthopedic Research Society*, Vol. 33, pp. 265, 1987.
- [16] Laine, A. & Fan, J, "Texture classification by wavelet packet signatures," *IEEE Transaction PAMI*, Vol. 11, pp. 1186-1191, 1993.
- [17] Unser, M, "Texture classification and segmentation using wavelet frames," *IEEE Transaction on Image processing*, Vol. 11(4), pp. 1549-1560, 1995.
- [18] Bullmore, E, Fadili, J, Maxim, V, Xendur, L, Mhitcher, B, Suckling, J, Brammer, M. J and Breakspear, M. J, "Wavelets and functional magneti resonance imaging of the human brain," *NeuroImage*, Vol 23, pp.234-249, 2004.
- [19] Lee W. L, Chen Y. C and Hsieh K. S, "Ultrasonic liver tissues classification by fractal feature vector based on M-band wavelet transform," *IEEE Trans. Med. Imag*, Vol. 22(3), pp. 382-392.
- [20] Faber T. D., Yoon D. C., Service S. K. & White S. C, "Fourier and wavelet analyses of dental radiographs detect trabecular changes in osteoporosis," *Bone*, Vol. 35(2), pp. 403-411, 2004.
- [21] Jakubas-Przewlocka J., Sawicki A. and Przewlocki P, "Assessment of trabecular bone structure in postmenopausal and senile osteoporosis in women by image analysis," *Scandinavian Journal of Rheumatology*, Vol. 32, pp. 295-299, 2003.
- [22] Jesu Christopher J, and Ramakrishnan S, "Assessment and classification of mechanical strength of human femur trabeculae bone using texture analysis and neural networks," *Journal of Medical System, Springer Publishers*, Vol. 35, pp.117-122, 2007.
- [23] Singh, M., Nagarath, A.R. and Maini, P.S, "Changes in trabecular pattern of the upper end of the femur as an index of osteoporosis," *Journal of Bone and Joint Surgery*, Vol. 52, pp. 457- 467, 1970.
- [24] Stiehl J B, Jacobson D, Carrera G, "Morphological analysis of the proximal femur using quantitative computed tomography," *Int orthop*, Vol. 31(3), pp.287-92, 2007.
- [25] Smith M. J and Barewell T. P, "Exact reconstruction techniques for tree structured subband coders," *IEEE Trans.Acoust., Speech, Signal Process.*, Vol. 34, pp. 434 441,1986.
- [26] Daubechies, I, "Ten lectures on wavelets," *Society for Industrial and Applied Mathematics, Philadelphia*: 1992.
- [27] Goldstein, S.A, "The mechanical properties of trabecular bone: dependence on anatomic location and function," *J. Biomech*, Vol. 20, pp. 1055-1061, 1987.
- [28] Goulet R.W, Goldstein S.A, Ciarelli M. J, Kuhn J. L, Brown M.B and Feldkamp L.A , "The relation between the structural and orthogonal compressive properties of trabecular bone," *J. Biomech*, Vol. 27, pp. 375-389, 1994.
- [29] Faulkner K.G, Gluer C.C, Majumdar S, Lang P, Engelke K and Genant H.K., "Noninvasive measurements of bone mass, structure and strength: current methods and experimental techniques," *AJR* , Vol. 157, pp. 1229-1237, 1991.
- [30] Link T.M., Majumdar S, Grampp S, Guglielmi G, van Kuijk C, Imhof H, Gluer C and Adams J.E, "Imaging of trabecular bone structure in osteoporosis," *European Journal of Radiology*, Vol. 9, pp. 1781-1788, 1999.
- [31] Pothuau L, Porion P, Lespessailles E, Benhamou C.L and Levitz P, "A new method for three-dimensional skeleton graph analysis of porous media: application to trabecular bone microarchitecture," *Journal of Microscopy*, Vol. 199, pp 41- 161, 2000.